

Solution Structure of pA2, the Mimotopic Peptide of Apolipoprotein A-I, by NMR Spectroscopy

Hoshik Won

*Department of Applied Chemistry, Hanyang University, Ansan 426-791, Korea. *E-mail: hswon@hanyang.ac.kr
Received July 31, 2011, Accepted September 20, 2011*

A number of mimetic peptides of apolipoprotein A-I, a major component for high density lipoproteins (HDL), were screened from the phase-displayed random peptide library by utilizing monoclonal antibodies (A12). A mimetic peptide for A12 epitope against apolipoprotein A-I was selected as FVLVRDTFPSSVCCP(pA2) exhibiting 45% homology with Apo A-I in the BLAST search. Solution structure determination of this mimotope was made by using 2D-NMR data and NMR-based distance geometry (DG)/molecular dynamic calculations. The resulting DG structures had low penalty value of 0.4-0.6 Å² and the total RMSD of 0.7-1.7 Å. The mimotope pA2 exhibited a characteristic β -turn conformation from Val[2] to Phe[8] near Pro[9] residue.

Key Words : Apolipoprotein A-I, NMR spectroscopy, Molecular dynamic computation

Introduction

Apolipoproteins playing an important role in lipid transport and metabolic process in blood stream are components of LDL and HDL. Based on the ABC nomenclature, apolipoproteins are classified into A-I, A-II, B, C-I, C-II, D, E, respectively. There are three main lipoprotein classes according to its density: very low density lipoproteins (VLDL), low density lipoproteins (LDL, $d = 1.019$ - 1.063 g/mL) and high density lipoproteins (HDL, $d = 1.063$ - 1.21 g/mL).^{1,2}

The structural modifications of apolipoprotein are known to be more important than that of blood serum and lipid-protein in the disease diagnosis of circulatory system. The change of apolipoprotein became an important estimation factor. As an example, the ratio apo A-I/apo B-100 is now often used as index causing the disease of coronary arteries.^{2,3}

Biochemical studies relating to the structure and metabolism of LDL received a great attention because there is the direct correlation between atherosclerosis and high LDL levels in human plasma. Low density lipoproteins are known to be the catabolic end product of VLDL and the major cholesterol-transporting lipoprotein in human plasma.² The majority of LDL particles contain a single apolipoprotein called apo B-100.³ After the elucidation of the role of apolipoproteins in the regulation of lipoprotein metabolism, it became apparent that improvements in the characterization of apo B-100 were needed to facilitate the development of the linkage between LDL and atherosclerosis.²

The profile is different from that of a typical apolipoprotein which has a high α -helical content and almost no β -sheet. In most apolipoproteins lipid binding occurs through amphipathic α -helical segment.⁴⁻⁶ The structure of human apo B has been analyzed in term of its functions in lipid binding, lipoprotein assembly and as the ligand responsible

for LDL clearance by the LDL receptor pathway.⁶ In apo B-100 few of the predicted α -helices are truly amphipathic in terms of charge distribution on the polar surface except for one extended region (residues 2,000-2,600) which contains good examples of amphipathic α -helices, and may contribute to lipid binding.⁴

HDL is a heterogeneous mixture of lipoprotein particles. The major protein component (~70%) of HDL is apo A-I carrying 243 amino acids synthesized in the small intestine and liver. The structure of truncated human apolipoprotein A-I, the major protein component of high density lipoprotein, has been determined at 4-Å resolution.⁷ Although the function of the apo A-II (ca 30% of apo A) is not clearly known, but some clinical results indicated that the apo A-I activates the lecithin cholesterol acyltransferase (LCAT) enzyme to remove the content of cholesterol in peripheral liver tissue. The level of apo A-I in HDL of cell plasma is responsible for the level of cholesterol. The results of clinical trials clearly have demonstrated that elevated high density lipoprotein levels strongly correlated with reduced risks of HDL to prevention of atherosclerosis is consonant with its role as the mediator of reverse transport of cholesterol for peripheral to the liver for catabolism.⁸ Hydrodynamics, electron microscopy and small angle X-ray scattering methods showed that spherical HDL consists of an ~84 Å diameter, core of neutral lipids and phospholipids acyl chains, surrounded by ~12 Å thickness of phospholipid head groups and protein.⁹ The C-terminal of apo A-I consists of vertically repeating units of amphiphilic helical structures, 11 or 2 × 11 amino acids in length, nestled between the phospholipid head groups exhibiting a strongly binding affinity to lipid, and this enhance the conversion of nascent discoidal HDL to spherical HDL particle by action of lecithin cholesterol acyltransferase.¹⁰

Conformational studies for mimetic peptide FVLVRDTFPSSVCCP(pA2) recognized by the monoclonal antibodies

providing the regulation of surface conformational change are designed based on the screening from the phase-displayed random peptide library by utilizing monoclonal antibodies (A12). These mimotopes were chemically synthesized and conjugated with carrier protein. The conjugated mimetic peptides were injected into Balb/c mice, and evaluated for the immunogenicity on the corresponding apolipoproteins. Immunochemical tests with the resulting anti-sera strongly suggested that the mimotopes were immunogenic and thus could be used as antigens for the induction of humoral immune responses to the lipoproteins. Mimotopes can be used as an alternative antigen as a constrained templates and results of detail biochemical tests will be published elsewhere.

The conformation of this mimotopic peptide pA2 may enhance to provide the new insights for the vaccine improvements in potency, specificity and safety. For NMR based structure determination and complete NMR signal assignments of this mimetic peptide, ^1H , ^{13}C , DEPT and 2D NMR experiments were performed. On the basis of distance data from NOESY experiments, distance geometry (DG) and molecular dynamics (MD) were carried out to obtain the tertiary structure of pA2 of the mimotop apolipoprotein A-I.

Methods

Preparation of Sample. A mimetic peptide FVLVRD-TFPSSVCCP(pA2) was obtained from Bio-Synthesis, Inc. Peptide was synthesized using solid-phase method (Fmoc chemistry). The water insoluble pA2 peptide was dissolved at 2.5 mM concentration in 350 μL DMSO- d_6 for NMR experiments.

NMR Measurements. All NMR experiments were performed by using the Varian Mercury 300 MHz and Unity INOVA 500 MHz NMR spectrometer. Two-dimensional NMR experiments included correlated spectroscopy (COSY) and such as the phase sensitive total coherence spectroscopy (TOCSY), nuclear Overhauser enhancement spectroscopy (NOESY) experiments were performed with a 256×2048 data matrix size with 16 scans per t1 increment and spectra were zero filled of 2048×2048 data points. TOCSY spectrum was collected with a mixing time of 50 msec, MLEV-17 spin lock pulse sequence. All of NMR data were processed by Varian VNMRJ and analyzed by using NMRView.¹¹

Determination of Solution State Structure. Structure determinations were carried out using HYGEOTM, HYNMRTM. Sequential assignments of amino acid spin systems were made using COSY, NOESY and TOCSY. Most important, direct way for secondary structure determination based on qualitative analysis of NOESY spectrum.¹² The structures were calculated from the NMR data according to the standard HYGEOTM simulated annealing and refinement protocols with minor modifications. NOE cross peaks were grouped according to their intensity into four categories: strong (2.0-3.0 Å), medium (2.0-3.5 Å),

weak (3.0-4.5 Å), and very weak (3.5-5.0 Å).

General ways of distance geometry (DG) algorithm accepts the input of distance constraints from NOE measurements.¹³ Set of distance restraints or bounds obtained from NOE data are determined by planarity restraints derived from the primary structure. This involves the selection of the possible intervals between lower and upper bounds consistent. After internal coordinates are embedded in space, the values of the distances within the bounds obtained by bound smoothing are guessed at random, and the atomic coordinates representing the best-fit to this guess are generated. The deviations of the coordinates from the distance bounds, as well as the stereospecific assignments, are minimized by lowering penalty values. When additional conjugate gradient minimization (CGM) was unable to further reduce the penalty for a particular structure, 2D NOESY back calculation were performed, and new distance restraints dictated by discrepancies between the experimental and back-calculated spectra were added to the experimental restraint list. Freshly embedded DG structures minimized with the modified restraints list generally exhibited penalty values lower than those of the previously refined structures and the new DG structures generally gave back-calculated NOESY spectra that were more consistent with experimental data.¹⁴ The structure was calculated using the DG algorithm HYGEOTM, and 10 separated structures were generated using all the constrains and random input. No further refinement by energy minimization was carried out on the output of the DG calculations. RMSD (root-mean-square distances) deviations between the NMR structures were 0.7-1.7 Å for the entire backbone.¹³ Back-calculation were assigned to GENNOE calculation in order to generate the theoretical NOEs. A consecutive serial files, obtained from GENNOE calculation, were incorporated into HYNMRTM to generate NOE back-calculation spectra which can be directly compared with experimental NOESY spectra.¹⁵

Results and Discussion

Connectivities derived from through bond J-coupling and through space coupling are important in NMR signal assignment and solution state structure determination. The ^1H - ^1H connectivities that identify the different amino acid type are established via scalar spin-spin coupling, using COSY and TOCSY. Assignments using sequential NOEs can be obtained for proteins with natural isotope distribution in space. Relations between protons in sequentially neighboring amino acid residues i and $i+1$ are established by NOEs manifesting close approach among d_{GN} , d_{NN} , d_{BN} . Except for flexible terminal amino acid residue Pro[15], complete NMR signal assignments listed in Table 1 were accomplished by utilizing homonuclear J-resolved 2D NMR experiments. The correlating signals of adjacent residues on the basis of dipolar connectivities obtained from 2D NOE spectra are listed in Table 2. Important NOEs are classified as strong(s), medium(m), weak(w), respectively, for NOE restraints in solution state structure determination. Dipolar

Table 1. ¹H-NMR Chemical Shift Assignments of pA2

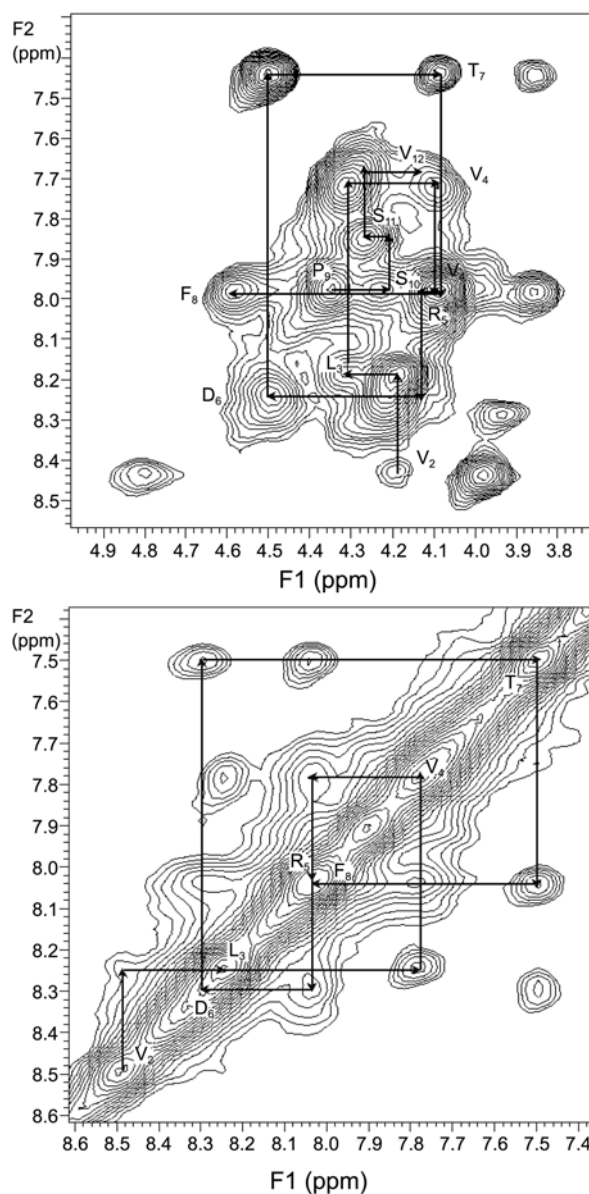
Residue	NH	α H	β H	γ H	Others
Phe[1]	8.041	4.450	2.795, 3.019		ring : 7.109
Val[2]	8.427	4.182	1.887	0.791	
Leu[3]	8.171	4.313	1.517	1.404	δ H : 0.778
Val[4]	7.722	4.076	1.914	0.757	
Arg[5]	7.967	4.206	1.627	1.425	δ H : 2.990, ϵ H : 7.638
Asp[6]	8.216	4.495	2.484, 2.508		
Tyr[7]	7.433	4.084	3.856	0.877	
Phe[8]	7.969	4.578	2.741, 2.946		ring : 7.199
Pro[9]	·	4.345	1.962	1.805	
Ser[10]	7.969	4.256	3.531, 3.581		
Ser[11]	7.842	4.270	3.531, 3.581		
Val[12]	7.667	4.146	1.927	0.757	
Cys[13]	8.232	4.715	2.726, 2.966		
Cys[14]	8.308	4.715	2.726, 2.966		
Pro[15]	·	4.345	1.962	1.805	

Table 2. Important NOE connectivities used for the structure determination of pA2

Residue	Chemical shift		NOE Connectivities
	(ppm)		
Phe[1] _{NH}	8.041	F _{1α} (w), F _{1β} (w)	
Phe[1] _{α}	4.450	F _{1β} (w)	
Val[2] _{NH}	8.427	V _{2α} (w), V _{2β} (vw), V _{2γ} (vw), L _{3NH} (w)	
Val[2] _{α}	4.182	L _{3NH} (s), V _{2β} (w), V _{2γ} (vw), R _{5NH} (w)	
Leu[3] _{NH}	8.171	L _{3α} (w), V _{2β} (w), L _{3β} (vw), L _{3γ} (m), L _{3δ} (w), V _{4NH} (s)	
Leu[3] _{α}	4.313	V _{4NH} (s), L _{3β} (vw), L _{3γ} (m), L _{3δ} (w), R _{5NH} (w)	
Val[4] _{NH}	7.722	V _{4α} (m), V _{4β} (m), V _{4γ} (m), L _{3β} (w), L _{3γ} (m), R _{5NH} (m)	
Val[4] _{α}	4.076	R _{5NH} (s), V _{4β} (m), R _{5γ} (w), V _{4γ} (m), D _{6NH} (w), T _{7NH} (w)	
Arg[5] _{NH}	7.967	V _{4β} (m), R _{5β} (w), R _{5γ} (m), V _{4γ} (m), D _{6NH} (m)	
Arg[5] _{α}	4.206	D _{6NH} (w), R _{5δ} (w), R _{5β} (m), R _{5γ} (m), F _{8NH} (w)	
Arg[5] _{δ}	2.990	R _{5β} (m), R _{5γ} (s), R _{5ϵ} (w)	
Asp[6] _{NH}	8.216	D _{6β} (m), R _{5β} (w), R _{5γ} (w), T _{7NH} (s)	
Asp[6] _{α}	4.495	T _{7NH} (s), D _{6β} (s), F _{8NH} (w)	
Tyr[7] _{NH}	7.433	T _{7β} (s), D _{6β} (w), R _{5γ} (vw), T _{7γ} (w), F _{8NH} (s)	
Tyr[7] _{α}	4.084	F _{8NH} (s), F _{8β} (s), T _{7γ} (s), S _{10NH} (w)	
Phe[8] _{NH}	7.969	F _{8β} (m), T _{7β} (s), T _{7γ} (m)	
Phe[8] _{α}	4.578	F _{8β} (w), P _{9γ} (vw)	
Pro[9] _{α}	4.345	P _{9β} (s), P _{9γ} (s), S _{10NH} (s)	
Pro[9] _{δ}	3.526	P _{9β} (w), P _{9γ} (s)	
Ser[10] _{NH}	7.969	S _{10α} (s), S _{10β} (s), P _{9β} (w), P _{9γ} (w), S _{11NH} (w)	
Ser[10] _{α}	4.256	S _{11NH} (m), S _{10β} (w), C _{13NH} (w)	
Ser[11] _{NH}	7.842	S _{11α} (s), S _{11β} (m), V _{12NH} (w)	
Ser[11] _{α}	4.270	V _{12NH} (m), S _{11β} (m), F _{8NH} (s), C _{14NH} (w)	
Val[12] _{NH}	7.667	V _{12α} (m), V _{12β} (w), C _{13NH} (w)	
Val[12] _{α}	4.146	V _{12β} (w), V _{12γ} (w)	

*Important NOEs are classified as strong(s), medium(m), weak(w), respectively, for NOE restraints in structure determination.

connectivities from amide protons to α - and amide protons were also used for sequential signal assignments, and the fingerprint region of the NOESY spectra recorded at 300 ms are shown in Figure 1. Connectivities of intraresidual cross peaks labeled in the NH-C α H region from Val[2] to Val[12], and NH-NH region from Val[2] to Tyr[7] of the NOESY spectra of pA2. Although the first residue Phe[1] and the last two residues Cys[14] and Pro[15] were not clearly showing inter-residual NOE connectivities, however important NOEs exhibiting peptide skeleton and specific conformation of mimetic peptide pA2 are observed to be Val[2] _{α} -Arg[5]_{NH}, Leu[3] _{α} -Arg[5]_{NH}, Val[4] _{α} -Asp[6]_{NH}, Val[4] _{α} -Tyr[7]_{NH}, Arg[5] _{α} -Phe[8]_{NH}, Asp[6] _{α} -Phe[8]_{NH}, Tyr[7] _{α} -Ser[10]_{NH}, Ser[10] _{α} -Cys[13]_{NH}, Ser[11] _{α} -Cys[14]_{NH}. In α -helical peptide conformation, proline enhances to form turn structure. Out of

**Figure 1.** Intraresidual cross peaks labeled in the NH-C α H region (upper), NH-NH region (lower) of the NOESY spectra of pA2 (τ_m = 300 ms).

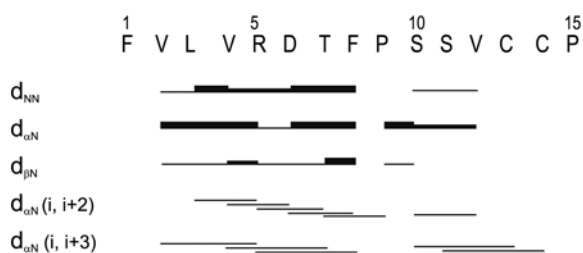


Figure 2. NOESY connectivity table of pA2: NOESY connectivities involving backbone protons for amino acids *i* and *j*. The height of the bars symbolizes the relative strength (strong (■), medium (▬), weak (—)) of the cross peaks in a qualitative way.

mimotope pA2 FVLVRDTPSSVCCP residues Val[2]_β-Phe[8]_{NH} demonstrates such a general tendency. By utilizing distance geometry and molecular dynamic computations incorporated with 2D NOE back calculations enable to confirm β-turn conformation. Intraresidual cross peaks labeled in the NH-C_αH region and NH-NH region clearly showed sequential connectivities and spatial conformation. Unfortunately important NOEs were not observed for Cys[14] and flexible terminal region Pro[15] due to serious signal overlap and residual flexibility. NOESY connectivities involving backbone protons for amino acids and the relative strength (strong, medium, weak) of the cross peaks in a qualitative way are shown in Figure 2. Although relatively weak *d*_{αN}(*i*, *i*+2) dipolar connectivities from residue number 2 to 8 were observed as shown in Figure 2, it was apparent that the mimotopic peptide pA2 has a characteristic β-turn conformation from Val[2] to Phe[8] near Pro[9] residue.

In order to determine the DG structure, several variable velocity simulated annealing and conjugate gradient minimization steps were used in the refinement scheme. Addition of restraints to account for minor differences between experi-

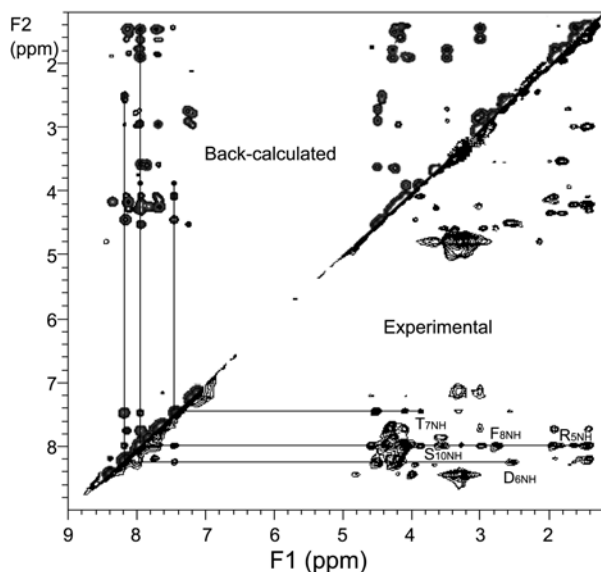


Figure 3. Comparisons of back-calculated and experimental NOESY spectrum of pA2 recorded at 300ms mixing time.

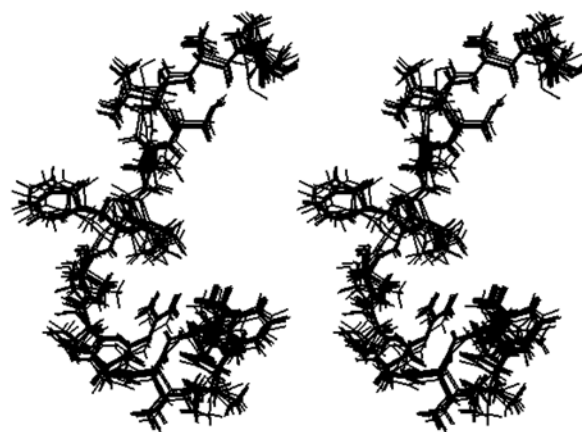


Figure 4. Stereoviews of pA2 showing best-fit superpositions of 10 NMR based solution structures with 0.7-1.7 Å RMSD (root-mean-square distances) deviations for entire skeleton.

mental and back-calculated spectra enabled the generation of new DG structures with substantially reduced penalties. To determine which of the DG structures most accurately reflect the experimental NOESY data, 2D NOESY back calculations were carried out. As illustrated in Figure 3, back-calculated spectrum of the pA2 was mostly consistent with the experimental NOESY data. Selected residual NOE connectivities of Arg[5]_{NH}, Asp[6]_{NH}, Phe[8]_{NH} and Ser[10]_{NH} were labeled for spectral comparisons. Ten final superimposed DG structures are shown in Figure 4. Pairwise RMSDs obtained upon superposition of all atoms were in the range 0.7-1.7 Å. The final result of a structure determination is presented as a superposition of a group of conformers for pairwise minimum root mean square deviation (RMSD) relative to a predetermined conformer. Although the incorporation of iterative 2D-NOE back calculations in structure determination gives optimal conformation that satisfies experimental NOEs, insufficient NOEs originated from flexible terminal residues Phe[1] and Pro[15] from repeating Cys[13] and Cys[14] resulted in relatively high RMSD values up to 1.7 Å in this study.

Conclusion

NMR signal assignments of potent mimetic peptide FVLVRDTPSSVCCP (pA2) were made by using homo nuclear correlation 2D NMR experiments including COSY, TOCSY and NOESY. Dipolar connectivities from amide protons to α- and amide protons were used for sequential signal assignments. Important NOEs exhibiting peptide skeleton and specific conformation of mimetic peptide pA2 are observed to be Val[2]_α-Arg[5]_{NH}, Leu[3]_α-Arg[5]_{NH}, Val[4]_α-Asp[6]_{NH}, Val[4]_α-Tyr[7]_{NH}, Arg[5]_α-Phe[8]_{NH}, Asp[6]_α-Phe[8]_{NH}, Tyr[7]_α-Ser[10]_{NH}, Ser[10]_α-Cys[13]_{NH}, Ser[11]_α-Cys[14]_{NH}. NMR based solution structures were determined with these important NOEs and 2D-NOE back calculation method. Out of mimotope pA2 FVLVRDTPSSVCCP residues Val[2]_β-Phe[8]_{NH} clearly demonstrate a β-turn conformation, as shown in Figure 5.

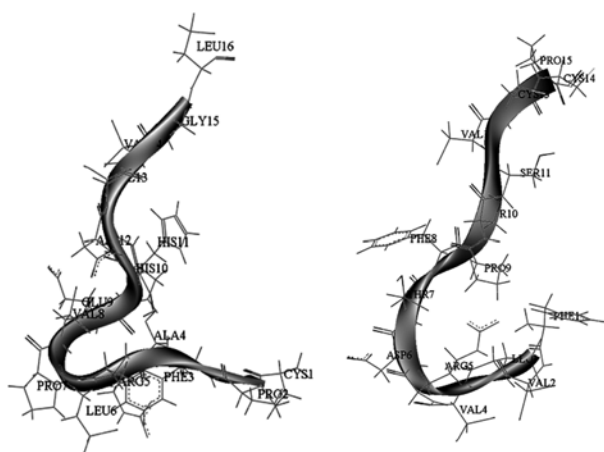


Figure 5. Comparisons of NMR based solution structure of mimetic peptide pA1(left) exhibiting a characteristic α -turn conformation from Leu[6] to His[11] and pA2(right) exhibiting a characteristic β -turn conformation from Val[2] to Phe[8].

Important NOEs exhibiting peptide skeleton and specific conformation of mimetic peptide CPFARLPVEHHDVVGL (pA1) were observed to be Ala[4] β -His[11] NH , Pro[7] α -Glu[9] NH , Val[8] α -His[10] NH , Glu[9] NH -His[11] NH , Asp[12] α -Val[14] NH in previous structural studies.¹⁶ Out of mimotope pA1 residues Ala[4] β -His[11] NH demonstrates α -helical peptide conformation that Pro[7] enhances to form a turn structure. Although relatively weak $d_{\alpha\text{N}}$ (i, i+2) dipolar connectivities from residue number 7 to 11 were observed, it was apparent that the mimotopic peptide pA1 has a characteristic conformation including a β -turn from Pro[7] to His[11].

As a result of NMR based structure determination of mimetic peptides pA1 and pA2, it was found that two highly potent mimetic peptides have a characteristic β -turn structure possibly derived from the proline in the middle of sequences as compared in Figure 5. It is believed that this interesting β -turn structure may play important role in the

recognition of the monoclonal antibodies. Future molecular docking studies with current results may provide the regulation of surface conformational changes in the mechanism of apolipoproteins playing an important role in lipid transport and metabolic process in blood stream are components of LDL and HDL.

References

1. Cruzado, I. D.; Cockrill, S. L.; McNeal, C. J.; Macfarlane, R. D. *J. Lipid Res.* **1998**, *39*, 205.
2. Mahley, R. W.; Innerarity, T. L.; Rall, S. C., Jr.; Wesgraber, K. H. *J. Lipid Res.* **1984**, *25*, 1277.
3. Davis, R. A. *Biochemistry of Lipids, Lipoproteins and Membranes*; Elsevier Science Publishers: Canada, 1991.
4. Segrest, J. P.; Jackson, R. L.; Morrisett, J. D.; Gotto, A. M. *FEBS Lett.* **1974**, *38*, 347.
5. Kaiser, E. T.; Kezdy, F. J. *Science* **1984**, *223*, 249.
6. Knott, T. J.; Pease, R. J.; Powell, L. M.; Wallis, S. C.; Rall, S. C., Jr.; Innerarity, R. L.; Blackhart, B.; Taylor, W. H.; Marcel, Y.; Milne, Y.; Johnson, D.; Fuller, M.; Lusic, A. J.; McCarthy, B. J.; Mahley, R. W.; Levy-Wilson, B.; Scott, J. *Nature* **1986**, *323*, 734.
7. Borhani, D. W.; Rogers, D. P.; Engler, J. A.; Brouillette, C. G. *Proc. Natl. Acad. Sci. U. S. A.* **1997**, *94*, 12291.
8. Castelli, W. P.; Garrison, R. J.; Wilson, P. W. F.; Abbott, R. D.; Kalousdian, S.; Kannel, W. B. *J. Am. Med. Assoc.* **1986**, *256*, 2835.
9. Atkinson, D.; Davis, M. A. F.; Leslie, R. B. *Proc. R. Soc. London* **1974**, *186*, 165.
10. Segrest, J. P.; Jones, M. K.; De Loof, H.; Brouillette, C. G.; Venkatachalapathi, Y. V.; Anantharamaiah, G. M. *J. Lipid Res.* **1992**, *33*, 141.
11. Johnson, B. A.; Blevins, R. A. *J. Biomol. NMR* **1994**, *4*, 603.
12. Wüthrich, K. *NMR of Proteins and Nucleic Acids*; Wiley: New York, 1986.
13. Evans, J. N. S. *Biomolecular NMR Spectroscopy*; Oxford Univ. Press: 1995.
14. South, T. L.; Blake, P. R.; Hare, D. R.; Summers, M. F. *Biochemistry* **1991**, *30*, 6342.
15. Kim, D.; Rho, J.; Won, H. *J. Korean. Mag. Reson. Soc.* **1999**, *3*, 44.
16. Kim, H.; Won, H. *Bull. Korean Chem. Soc.* **2011**, *9*, 3425.